

RESEARCH ARTICLE

Potential matrix metalloproteinase-9 inhibitor of aurone compound isolated from *Sterculia quadrifida* leaves: *In-vitro* and *in-silico* studies

Rollando Rollando^{1,2*}, Warsito Warsito², Masruri Masruri², Nashi Widodo³

¹Pharmacy Department, Faculty of Science and Technology, Ma Chung University, Malang 65151, Indonesia.

²Doctoral Student, Chemistry Department, Faculty of Mathematics and Natural Sciences, Brawijaya University, Malang 65145, Indonesia.

³Chemistry Department, Faculty of Mathematics and Natural Sciences, Brawijaya University, Malang 65145, Indonesia.

⁴Biology Department, Faculty of Mathematics and Natural Sciences, Brawijaya University, Malang 65145, Indonesia.

*Corresponding Author E-mail: ro.llando@machung.ac.id

ABSTRACT:

In our previous study, aurone compound were found in the n-butanol fraction of *Sterculia quadrifida* leaves. The aurone compound (compound 1) had high cytotoxic activity in cell lines with IC₅₀ values of 4.05, 12.53, 15.38, and 25.91 µg/mL in 4T1, MCF7, MDA-MB-435, T47D, respectively. In this study, we performed the MMP-9 enzyme inhibition test with FRET assay, and to deepen the mechanism of action of the compounds use molecular docking and molecular dynamics. The results showed that compound 1 had the MMP-9 enzyme inhibition of 91.23% and IC₅₀ 48.27%. Furthermore, molecular docking and molecular dynamic simulation suggest compound 1 interacts firmly and stably at the enzyme catalytic site. In conclusion, this study can provide important information on the development of herbal medicines that are potentially cancer drugs.

KEYWORDS: Aurone, MMP-9 assay, Molecular docking, Molecular dynamic simulation, RMSD, RMSF.

INTRODUCTION:

Breast cancer is cancer that causes the most deaths in women, with 1.2 million cases per year¹. Breast cancer is part of society's problems that require primary and secondary prevention globally². Early detection and treatment can reduce the risk of death from breast cancer³. The main cause of death and failure of breast cancer treatment is distant metastasis⁴. Triple-negative breast cancer has a close relationship with the metastatic process in breast cancer because it has a high invasive character and very high metastatic potential⁵. The process of metastatic cancer cells has a close relationship with protease enzymes secreted by cancer cells, one of which is the matrix metalloprotease enzyme⁶. MMP-9 has been reported as a potentially useful biomarker for the aggressive subtype of breast cancer⁷.

Currently, few drugs are used to inhibit MMP-9 selectively; therefore, it is necessary to explore chemical compounds to look for drugs that selectively inhibit the MMP-9 enzyme.

In our previous work, the compound (2E)-2-[(3,4-dihydroxy phenyl)(hydroxy)methylidene]-4,6-dihydroxy-2,3-dihydro-1-benzofuran-3-one (compound 1) has been isolated aurone compounds (Figure 1). Compound 1 was isolated from the n-butanol fraction from the leaves of *Sterculia quadrifida*. Compound 1 are reported to have high antioxidant, antibacterial, and cytotoxic activities. The antioxidant assay results showed IC₅₀ values of 46.36, 38.41, 37.85, and 20.50 µg/mL in the DPPH, ABTS, NO, and H₂O₂ assays, respectively. Then, the antibacterial assay results showed IC₅₀ values of 23.38, 26.22, 58.45, 100.92, 103.14, and 193.98 µg/mL in *P. aureginosa*, *H. pylori*, *S. bovis*, *S. aureus*, *S. thypi*, *E. coli*, respectively. After that, the cytotoxicity assay showed IC₅₀ values of 4.05, 12.53, 15.38, and 25.91 µg/mL in 4T1, MCF7, MDA-MB-435, T47D, respectively. In addition, when viewed from the

selectivity index (SI), the SI value in cell 4T1 is 10.68, cell MCF7 is 3.45, and cell MDA-MB-435 is 2.81. Compound 1 was proven to be non-toxic to Vero cells (normal cells) because the SI value was >2 . 4T1 cells are triple-negative breast cancer; interestingly, the cytotoxic test results of compound 1 in 4T1 cells showed very high test results and had the potential to be tested on MMP-9 enzymes⁸.

As a continuation of our previous research, this present study, an in-vitro test against MMP-9 based on Fluorescence Resonance Energy Transfer (FRET) assay was carried out based on the results of the cytotoxic test of aurone compounds on 4T1 and MDA-MB-435 cells, which represent breast cancer cells with the type triple-negative breast cancer. First, the test aimed to find the ability of the compound 1 to inhibit the MMP-9 enzyme in the hope of inhibiting the metastatic process of breast cancer cells. Then, an investigation was carried out using molecular docking and molecular dynamic simulation to explore the mechanism of the compound 1 at the active site of the MMP-9 enzyme.

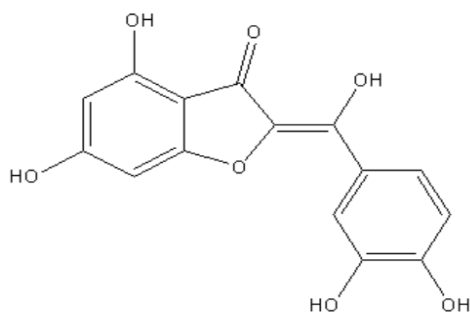


Figure 1. Chemical structure of compound 1 isolated from n-butanol fraction of *S. quadrifida* leaves

MATERIALS AND METHODS:

Materials:

Chemicals:

The aurone compounds (compound 1): (2E)-2-[(3,4-dihydroxy phenyl)(hydroxy)methylidene]-4,6-dihydroxy-2,3-dihydro-1-benzofuran-3-one were obtained from previous studies. The MMP9 enzyme kit was obtained from BioVision and comprised of lyophilized MMP-9, FRET-based MMP-9 substrate (Mca-Pro-Leu-Gly-Leu-Dpa-Ala-Arg), MMP-9 assay buffer, and NNGH inhibitor (N-isobutyl-N- (4- methoxyphenylsulfonyl)-glycyl hydroxyamic acid) as its positive control.

Software and hardware:

PEX9 1ITV were downloaded from the Protein Databank (PDB, www.rcsb.org), the molecular docking used Autodock Vina embedded in Pyrx 0.9.9 and the output was visualized using Biovia Discovery Studio 2016 (www.accelrys.com) and PyMol (www.pymol.org). An Lenovo laptop with Core i5

processor on a Windows 10 operating system with 8 GB RAM and 500 GB Hard Disk was the hardware.

Methods:

In vitro MMP-9 inhibition assay:

Lyophilized MMP-9 enzyme was reconstituted with 110 μ L 30% glycerol in deionized water. Then, 550 μ L of buffer for the enzyme was added, and it was ready for use. The sample was prepared by dissolving it in 1 μ L DMSO to obtain a stock concentration of 20.000 μ g/mL (ppm) in a microtube. The final concentration of DMSO in the well-plate was 1%. Blanks were prepared by adding 100 μ L of the MMP-9 test kit buffer to a 96-well plate. Then, 44 μ L of MMP-9 test buffer was added, 1 μ L compound solution, and 5 μ L of MMP-9 enzyme were added. The final concentration of the sample in the well was 200 μ g/mL. Solvent control was made by taking 40 μ L of MMP-9 test buffer, 5 μ L of solvent used (ethanol), and 5 μ L of MMP-9 enzyme. Negative control was made by pipetting 45 μ L of MMP-9 test kit buffer and 5 μ L of MMP-9 enzyme in wells. The positive control consisted of 43 μ L of MMP-9 test buffer, 2 μ L of NNGH, and 5 μ L of MMP-9 enzyme. Samples, blanks, solvent control, negative control, and positive control were incubated for 30 minutes at 37°C. After incubation, 1 μ L of FRET-based peptide MMP-9 substrate and 49 μ L buffer was added to the sample, solvent control, negative control, and positive control followed by incubation for 60 minutes at 37°C. Fluorescence was then read using Microplate Reader at 325/393 nm⁸.

Molecular docking:

The crystal structure of PEX9 was downloaded from the Protein Data Bank (PDB) with PDB ID 1ITV. Sulfate ion was used as the native ligand. The sulfate ion separated from PEX9 using PyMol. Polar hydrogen were retained with Kollman charges. Docking was performed with AutoDock Vina embedded in the PyRx 0.9.9 program with a grid (completeness = 8; sizes 25, 25, 25 and center x = -42.05, y = -30.82, z = -7.26). If the RMSD value is given to be less than 2Å, the docking is declared valid⁹.

Molecular dynamic simulation:

Molecular Dynamics (MD) simulation was carried out using YASARA Structure version 14.12.2 and run under Microsoft Windows 10 operating system. The force field used in this simulation is the YAMBER Force field. The Coulomb distance interaction is calculated using the Ewald particle algorithm, while the Van der Waals force is limited to 8 Å. Cube-shaped simulation box is placed around the simulated molecules at a distance of 5 nm. The size of the simulated box is 50 \times 50 \times 50 Å with a value of n = 6. The boundary of the simulated box is conditioned in periodic form. The water density was set

at 1 g/cc at 298 K. Simulations were run for 10 ns with photographs taken every 100 ps⁷.

RESULT:

MMP-9 in-vitro assay

Table 1. MMP-9 in-vitro test results

Compound	% Inhibition	IC ₅₀ (µg/mL)
Cisplatin	97,12	16,31
NNGH	96,82	4,09
Compound 1	91,23	48,27

The test results on the MMP-9 enzyme showed that Cisplatin had the highest inhibitory value of 97.12%, followed by NNGH (96.82%) and compound 1 (91.23%). Then, when observed from the concentration of compounds that can inhibit the MMP-9 enzyme, NNGH as a control inhibitor of the MMP-9 enzyme has the highest IC₅₀ value of 4.09 µg/mL and compound 1 with a value of 48.27 µg/mL. Furthermore, the statistical analysis results on the IC₅₀ value showed that the IC₅₀ value had a significant difference with NNGH (Table 1).

Molecular docking:

Molecular docking results showed that the sulfate ion as a control ligand had an RMSD of 0.7 Å (less than 2 Å), indicating that the molecular docking parameters were reproducible^{9,10}. Table 2 shows the range of free energy (ΔG_{bond}) between -3.5 to -6.2 kcal/mol. The results of the analysis showed that NNGH as a positive control had the highest bond energy (-6.2 kcal/mol), followed by compound 1 (-3.4 kcal/mol) and sulfate ion (-3.5 kcal/mol). The free energy shows that NNGH has a stronger interaction as an inhibitor of the MMP-9 enzyme compared to compound 1. In this study, the molecular docking test results positively correlate with the in vitro test results, and it can be seen that NNGH has the highest free energy bond and MMP-9 enzyme inhibitory activity.

Table 2. Compound bonding affinity, interactions, and amino acid residues

Ligand	Free energy bond (kcal/mol)	Hydrogen bond	Hydrophobic interaction
Sulfate ion (native ligand)	-3,5	Glutamic acid60, glycine154, glutamic acid14	Phenylalanine59, alanine13
NNGH	-6,2	Glutamic acid14, glutamic acid157, glutamine154, glutamic acid60, arginine106	Methionine112, phenylalanine59, alanine104, valine158, phenylalanine153, valine152, glycine16
Compound 1	-3,4	Serine107, valine170,	Phenylalanine142, leucine113,

		alanine159, glutamic acid157	glutamine154, arginine106, asparagine177, serine171, serine172, lysine158, glycine108
--	--	------------------------------	---

The MMP-9 enzyme has a catalytic domain (active site) in the A chain with important amino acids that generate the stimulus, namely glutamic acid14, arginine106, and glutamic acid157^{11,12}. From the results of the molecular docking (Figure 2), the sulfate ion compound, which is the control ligand, establish hydrogen bonds with the amino acids glutamic acid60, glycine154, glutamic acid14, and can establish hydrophobic bonds with the amino acids phenylalanine59 and alanine13. Then, NNGH can form hydrogen bonds with the amino acids glutamic acid14, glutamic acid157, glutamine154, glutamic acid60, arginine106, and form hydrophobic interactions with the amino acids methionine112, phenylalanine59, alanine104, valine158, phenylalanine153, valine152, and glycine16. Then, compound 1 was seen to establish hydrogen bonds with compounds serine107, valine170, alanine159, glutamic acid157, and hydrophobic interactions with compounds phenylalanine142, leucine113, glutamine154, arginine106, asparagine177, serine171, serine172, lysine158, and glycine108. From the observation of hydrogen bonds and hydrophobic interactions, it is seen that the test compound can establish hydrogen bonds and hydrophobic interactions with important amino acids in the catalytic domain of the MMP-9 enzyme.

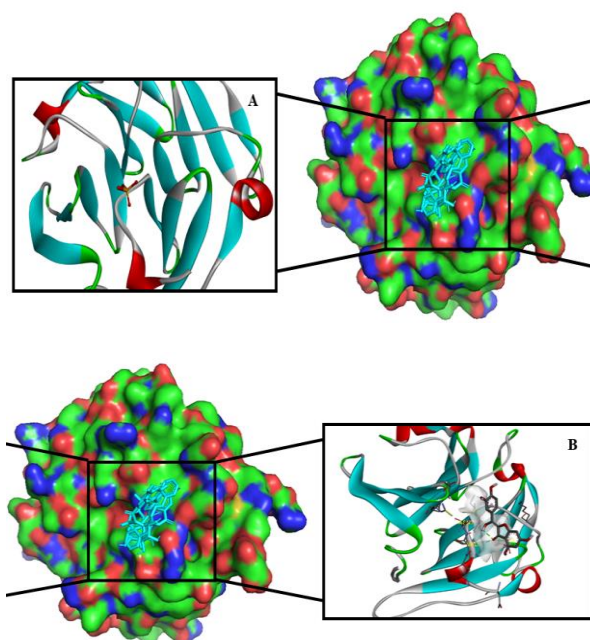


Figure 2. The docking pose of (A) SO₄ ion, (B) compound 1

Molecular dynamic simulation:

The interactions between control ligand and compound 1 as inhibitors of the MMP-9 enzyme can be analyzed more deeply by using molecular dynamics simulation^{11,12}. First, the results of the analysis of the RMSD value of the protein-native ligand complex (SO₄) showed a deviation between 0.414 to 1.693 Å (Figure 3); when observed from the range of RMSD values the protein-native ligand complex, it can be concluded have stable interaction. Then, the results of the analysis of the RMSF value on the protein-native ligand complex showed a deviation between 0.43 to 2.68 Å. Based on the RMSF value of the native ligand, it can be concluded that the native ligand has stable interaction. After that, the results of the RMSD analysis on NNGH showed a deviation ranging from 0.383 to 1.641 Å (Figure 3). Then, the analysis of the RMSF value of the protein-NNGH complex showed a deviation range of 0.44 to 3.13 Å. The most significant deviation was seen in the protein-NNGH complex at residue 62, with a value of 3.13 Å during the 10 ns simulation. Finally, the analysis of the RMSD values in protein-compound 1 complex showed a deviation range from 0.412 to 2.225 Å, an increase in the RMSD value from 0.4 to 10 ns (Figure 3). Then, the results of the analysis of the RMSF value of protein-compound 1 complex showed a fluctuation of 0.42 to 3.45 Å; in the analysis of the RMSF value, there was a fluctuation of 3.45 Å at residue 14 and 2.93 Å at residue 89.

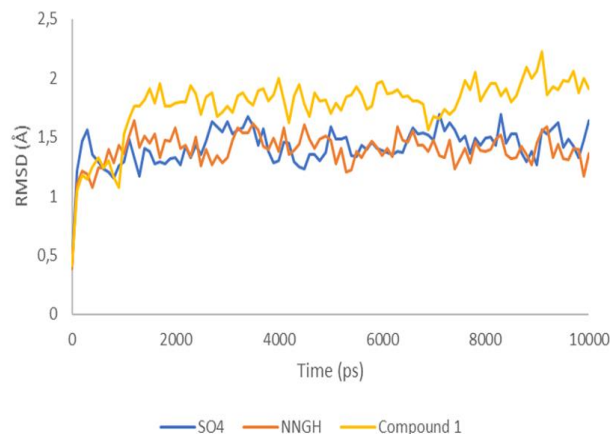


Figure 3. RMSD of sulfate ion (blue), NNGH (orange), compound 1 (yellow) for 10 ns molecular dynamics simulation, shown in 100 frames

DISCUSSION:

Matrix Metalloproteinase-9 (MMP-9) is a protein with protease activity, with the primary substrates being extracellular matrix and membrane attachment^{11,12}. This protein is one of the most important members of the matrix metalloproteinase family. It is a protein that can bind and digest collagen as the most important compound of the membrane. Several studies have

reported that changes in the expression of the MMP-9 protein may play an essential role in the differentiation and behavior of cancer cells¹³⁻¹⁵. Studies have demonstrated the role of MMP-9 in the initiation, proliferation, and metastasis of breast cancer cells through collagen digestion and interactions with tumor suppressor proteins¹⁶⁻¹⁸. Most importantly, inhibition of the MMP-9 protein is an essential step in reducing the survival and progression of breast cancer¹⁹⁻²¹.

Compound 1 is a flavonoid compound with the basic structure of an auron. In several studies that have been carried out, it is reported that flavonoid compounds have an activity to inhibit the MMP-9 enzyme. Wu. *et al.*²² reported that luteolin compounds have cytotoxic activity on MDA-MB-231, MDA-MB-486, 4T1, and BT-549 breast cancer cells with strong activity. In addition, luteolin has also been reported to downregulate MMP-9 expression by lowering AKT/mTOR levels that promote H3K27Ac and H3K56A in the MMP-9 promoter region. Later, herbacetin compounds have cytotoxic activity on A375 and Hs294T cells with strong activity.

Furthermore, it is said that herbacetin can suppress MMP-9 mediated angiogenesis by blocking the EGFR-ERK/AKT signaling pathway²³. The mechanism of inhibition of angiogenesis by flavonoid compounds of the auron group can also occur with other mechanisms, such as silibinin compounds which inhibit the migration and invasion of breast cancer cells MDA-MB-231 through the induction of mitochondrial fusion, mitochondrial fusion imbalance will inhibit the hippo pathway-YAP/TAZ and c-Jun pathway N-terminal kinase (JNK) so that the process of mitochondrial division and angiogenesis will be inhibited²⁴. In addition, it is also reported that pectolarigenin, which is administered intraperitoneally, can inhibit the metastasis of breast cancer cells type 4T1, MDA-MB-231, and MCF-7 in the lungs. These compounds can inhibit metastasis by downregulating phosphorylated Stat3- and expression of matrix metalloproteinases 2 and 9²⁵⁻²⁷.

CONCLUSION:

In-vitro and *in-silico* assays on compound 1 interacted strongly at the active site of the MMP-9 enzyme receptor and had a stable interaction with amino acids on the active site of the receptor with RMSD <2.

CONFLICT OF INTEREST:

The authors have no conflicts of interest regarding this investigation.

ACKNOWLEDGMENTS:

This article is part of the doctoral thesis and the research funded by Ma Chung Research Group Grant No:

002/MACHUNG/LPPM-MRGG/I/2021

REFERENCES:

- Sung H. Ferlay J. Siegel R.L. Laversanne M. Soerjomataram I. Jemal A. Bray F. Global Cancer Statistics 2020: GLOBOCAN Estimates of Incidence and Mortality Worldwide for 36 Cancers in 185 Countries. CA: a cancer journal for clinicians, 2021; 71(3): 209–249. doi.org/10.3322/caac.21660
- Latest global cancer data: Cancer burden rises to 19.3 million new cases and 10.0 million cancer deaths in 2020 QUESTIONS AND ANSWERS (Q&A) – IARC. (n.d.). Retrieved November 27, 2021, from <https://www.iarc.who.int/faq/latest-global-cancer-data-2020-qa/>
- Figueroa J.D. Gray E. Pashayan N. Deandrea S. Karch A.Vale D.B. Nickson C. The impact of the Covid-19 pandemic on breast cancer early detection and screening. Preventive Medicine. 2021; 151(1), 10-16. doi.org/10.1016/j.ypmed.2021.106585
- Zhang J. Wei Q. Dong D. Ren L. The role of TPS, CA125, CA15-3 and CEA in prediction of distant metastasis of breast cancer. Clinica Chimica Acta. 2021; 523(3), 19–25. doi.org/10.1016/j.cca.2021.08.027
- Yin L. Duan J.J. Bian X.W. Yu S.C. Triple-negative breast cancer molecular subtyping and treatment progress. Breast Cancer Research: BCR. 2020; 22(1): 61-78. doi.org/10.1186/s13058-020-01296-5
- Gautam J. Banskota S. Lee H. Lee Y.J. Jeon Y.H. Kim J.A. Jeong B.S. Down-regulation of cathepsin S and matrix metalloproteinase-9 via Src, a non-receptor tyrosine kinase, suppresses triple-negative breast cancer growth and metastasis. Experimental & Molecular Medicine. 2018; 50(9):1–14. doi.org/10.1038/s12276-018-0135-9
- Hariono M. Rollando R. Karamoy J. Hariyono P. Atmono M. Djohan M. Wahab H. Bioguided fractionation of local plants against matrix metalloproteinase9 and its cytotoxicity against breast cancer cell models: in silico and in vitro study. Molecules.2020; 25(20). doi.org/10.3390/molecules25204691
- Rollando R. Warsito W. Masruri M. Widodo W. Sterculia foetida leaf fraction against matrix metalloproteinase-9 protein and 4t1 breast cancer cells: in-vitro and in-silico studies. Tropical Journal of Natural Product Research. 2021; 5(1): 113–121. doi.org/10.26538/tjnpr/v5i1.15
- Otuokere I.E. Amaku F.J. Alisa C.O. In silico geometry optimization, excited – state properties of (2e)-n-hydroxy-3-[3-(phenylsulfamoyl) phenyl] prop-2-enamide (belinostat) and its molecular docking studies with ebola virus glycoprotein. Asian Journal of Pharmaceutical Research. 2015; 5(3): 131-137. doi. 10.5958/2231-5691.2015.00020.9
- Rutuja P. P. Sachin H. R. Role of autodock vina in pyrx molecular docking. Asian Journal of Research in Chemistry. 2021; 14(2):132-134. doi: 10.5958/0974-4150.2021.00024.9
- Hariono M. Nuwarda R.F. Yusuf M. Rollando R. Jenie R.I. Al-Najjar, Wahab H.A. Arylamide as potential selective inhibitor for matrix metalloproteinase 9 (mmp9): design, synthesis, biological evaluation, and molecular modeling. Journal of Chemical Information and Modeling. 2020; 60(1): 349–359. doi.org/10.1021/acs.jcim.9b00630
- Xavier S.M. Mahalakshmi J.A. Vinisha G. Computational modeling of novel drug targets fitse and mpt83 for mdrtb and molecular docking of selected compounds from medicinal plants. Research Journal of Pharmacy and Technology. 2018; 11(4): 1413-1420. doi.10.5958/0974-360X.2018.00264.0
- Vijayakumar V. Radhakrishnan N. Vasantha-Srinivasan P. Molecular docking analysis of triazole analogues as inhibitors of human neutrophil elastase (hne), matrix metalloproteinase (mmp 2 and mmp 9) and tyrosinase. Research Journal of Pharmacy and Technology. 2020; 13(6): 2777-2783. doi.10.5958/0974-360X.2020.00493.X
- Skariyachan S. Gopal D. Chakrabarti S. Kempanna P. Uttarkar A. Muddebihalkar A.G. Niranjana V. Structural and molecular basis of the interaction mechanism of selected drugs towards multiple targets of SARS-CoV-2 by molecular docking and dynamic simulation studies- deciphering the scope of repurposed drugs. Computers in Biology and Medicine. 2020; 126(4):10-14. doi.org/10.1016/j.combiomed.2020.104054
- Dong H. Diao H. Zhao Y. Xu H. Pei S. Gao J. Lin D. Overexpression of matrix metalloproteinase-9 in breast cancer cell lines remarkably increases the cell malignancy largely via activation of transforming growth factor beta/SMAD signalling. Cell Proliferation. 2019; 52(5):25-34. doi.org/10.1111/cpr.12633
- Huang H. Matrix metalloproteinase-9 (mmp-9) as a cancer biomarker and mmp-9 biosensors: recent advances. Sensors. 2018;18(10):67-74. doi.org/10.3390/s18103249
- Aloss K. Jdeed S. Alshehbi. J. Detecting the role of CCR7-CCL21/CCL19 axis in breast cancer progression and lymph node metastasis incidence. Research Journal of Pharmacy and Technology. 2018; 11(1): 231-235. doi.10.5958/0974-360X.2018.00043.4
- Mohammadian H. Sharifi R. Rezanezhad A.S. Taheri E. Babazadeh B.A. Matrix metalloproteinase MMP1 and MMP9 genes expression in breast cancer tissue. Gene Reports. 2020; 21(5): 10-19. doi.org/10.1016/j.genrep.2020.100906
- Jainab N.H. Raja M.K.M.M. In silico molecular docking studies on the chemical constituents of clerodendrum phlomidis for its cytotoxic potential against breast cancer markers. Research Journal of Pharmacy and Technology. 2018; 11(4): 1612-1618. doi.10.5958/0974-360X.2018.00300.1
- Anggi V. Adikusuma W. Total antioxidant and in-vitro cytotoxic of *Abelmoschus manihot* (L.) medik from palu of central sulawesi and doxorubicin on 4T1 cells line and Vero cells. Research Journal of Pharmacy and Technology. 2019; 12(11): 5472-5476. doi.10.5958/0974-360X.2019.00949.1
- Novitasari D. Jenie R.I. Wulandari F. Utomo R.Y. Putri D.D.P. Kato J. Meiyanto E. Curcumin-like structure (CCA-1.1) induces permanent mitotic arrest (Senescence) on Triple-negative breast cancer (TNBC) cells, 4T1. Research Journal of Pharmacy and Technology. 2021; 14(8):4375-2. doi.10.52711/0974-360X.2021.00760
- Wu H.T. Lin J. Liu Y.E. Chen H.F. Hsu K.W. Lin S.H. Chen D.R. Luteolin suppresses androgen receptor-positive triple-negative breast cancer cell proliferation and metastasis by epigenetic regulation of MMP9 expression via the AKT/mTOR signaling pathway. Phytomedicine.2021; 81(3): 15-35. doi.org/10.1016/j.phymed.2020.153437
- Li L. Fan P. Chou H. Li J. Wang K. Li H. Herbacetin suppressed MMP9 mediated angiogenesis of malignant melanoma through blocking EGFR-ERK/AKT signaling pathway. Biochimie. 2019; 162(6):198–207. doi.org/10.1016/j.biochi.2019.05.003
- Si L. Fu J. Liu W. Hayashi T. Nie Y. Mizuno K. Ikejima T. Silibinin inhibits migration and invasion of breast cancer MDA-MB-231 cells through induction of mitochondrial fusion. Molecular and Cellular Biochemistry. 2020; 463(2):189–201. doi.org/10.1007/s11010-019-03640-6
- Li Y. Gan C. Zhang Y. Yu Y. Fan C. Deng Y. Yin W. Inhibition of stat3 signaling pathway by natural product pectolarigenin attenuates breast cancer metastasis. Frontiers in Pharmacology. 2019; 10(2): 89-95. doi.org/10.3389/fphar.2019.01195
- Firoj A.T. Harinath N. More inhibitory effects of successive solvent extracts of *Barleria gibsoni* Dalz. on the proliferation of MDA MB 4355 (human breast cancer) and Hep G2 (liver cancer cell line). Asian Journal of Pharmaceutical Research. 5(4): 2015; 183-185. doi.10.5958/2231-5691.2015.00028.3
- Lavanya M. Bhaumik A. Reddy A.G. Manasa H. Kalyani B. Sushmitha.S. Evaluation of anticancer activity of ethanolic and ethylacetate extracts of sweet cherry against human breast cancer cell line MCF-7. Research Journal of Pharmacology and Pharmacodynamics. 2016; 8(2): 65-70. doi. 10.5958/2321-5836.2016.00012.4